Photophysics and nonlinear absorption of 4,4′-diethynylazobenzene derivatives terminally capped with substituted aromatic rings

ARTICLE *in* JOURNAL OF PHOTOCHEMISTRY AND PHOTOBIOLOGY A: CHEMISTRY · JULY 2012

Impact Factor: 2.5 · DOI: 10.1016/j.jphotochem.2012.04.021

Journal of Photochemistry and Photobiology A: Chemistry 239 (2012) 47–54

Contents lists available at SciVerse ScienceDirect

Journal of Photochemistry and Photobiology A: Chemistry

journal homepage: www.elsevier.com/locate/jphotochem

Photophysics and nonlinear absorption of 4,4′-diethynylazobenzene derivatives terminally capped with substituted aromatic rings

Rui Liu[a,b], Yuhao Li[a,b], Jin Chang[b,c], Qi Xiao[b,c], Hongjun Zhu[b,**], Wenfang Sun[a,*]

[a] Department of Chemistry and Biochemistry, North Dakota State University, Fargo, ND 58108-6050, USA
[b] Department of Applied Chemistry, College of Science, Nanjing University of Technology, Nanjing 210009, PR China
[c] Discipline of Chemistry, Queensland University of Technology, 2 George St., Brisbane 4000, Australia

ARTICLE INFO

Article history:
Received 15 February 2012
Received in revised form 6 April 2012
Accepted 28 April 2012
Available online xxx

Keywords:
Azobenzene
Electronic absorption
Emission
DFT calculations
Transient difference absorption
Nonlinear absorption

ABSTRACT

The photophysical properties of a series of 4,4′-diethynylazobenzene derivatives terminally capped with substituted aromatic rings (**1a**: R = phenyl; **1b**: R = 4-(diphenylamino)phenyl; **1c**: R = 4-(9*H*-carbazol-9-yl)phenyl; **1d**: R = 9*H*-fluoren-2-yl; **1e**: R = biphenyl-4-yl; **1f**: R = naphthalen-2-yl) were systematically investigated. All compounds exhibit strong $^1\pi,\pi^*$ absorption bands in the UV region; and a broad, structureless charge-transfer band/shoulder in the visible region (except for **1a**), which systematically red-shifts when electron-donating substituents are introduced to the terminal phenyl rings, but blue-shifts when π-conjugation of the terminal aromatic ring increases. All compounds are emissive in solution at room temperature and at 77 K. When excited at the low-energy absorption band, the compounds emit fluorescence between 369 and 419 nm, which can be attributed to $^1\pi,\pi^*/^1$ICT (intramolecular charge transfer) state. Density functional theory (DFT) calculations on **1a**–**1f** in gas phase were also performed to gain insight into the nature of the ground electronic state and the low-lying excited electronic states. **1d**–**1f** exhibit strong triplet transient absorption band(s) in the visible spectral region, which are mainly attributed to the $^3\pi,\pi^*$ state. Reverse saturable absorption (RSA) of these compounds was demonstrated at 532 nm using ns laser pulses. The degree of RSA follows this trend: **1b** > **1c** ≈ **1a** > **1e** > **1f** > **1d**, which is mainly determined by the ratio of the triplet excited-state absorption cross-section to that of the ground-state and the triplet excited-state quantum yield.

1. Introduction

Azobenzene compounds have attracted a great deal of interest in recent years due to their intriguing photophysical properties and versatile applications in photo-responsive materials [1–6], supramolecular structure construction [7–10] and non-linear optics [11,12]. They can undergo reversible *trans*-to-*cis* transformation by illumination with UV/visible light, and the inverse *cis*-to-*trans* reaction can be achieved by irradiation with a different wavelength UV/visible light or by thermal relaxation. This alternation in structure causes a significant change in color, refractive index, dielectric constant, and dipole moment, *etc.*, which makes them attractive in the realms of functional materials [13–17].

Zeitouny and co-workers reported a series of ethynyl-bearing azobenzene compounds with peripheral groups that exhibit substantial *trans–cis* isomerization [17], and pyrene-centered molecular arachnoid with four azobenzenyl-ethynyl legs that show photoswitch ability and NIR emitting properties [18]. Tour's group has also developed a class of novel oligo(phenyleneethynylene)azobenzene derivatives as potential candidates for molecular electronic switching devices [19,20]. In addition, they incorporated the azobenzene group in a nanovehicle as photoactive moiety, which exhibits worm-like movement on a surface upon light irradiation [15].

Although the reported work is quite intriguing, the study on the effect of terminally capped chromophores on the photophysics, especially on the nonlinear absorption of phenyleneethynyleneazobenzene compounds is still quite limited. To remedy this deficiency, our group has designed and synthesized a series of 4,4′-diethynylazobenzene derivatives terminally capped with substituted aromatic rings (Chart 1). Compared to the reference compound **1a** with terminal phenyl group, NPh_2 and carbazolyl groups are chosen as electron-donating substituent on the phenyl ring and fluorenyl, biphenylyl and naphthyl groups are chosen as expanded π-electron systems to replace phenyl group in order to study the effect of electron donor and extended π-conjugation on the photophysics and nonlinear absorption of these compounds. Their photophysical properties were systematically investigated with the aim to provide a basis for elucidating

* Corresponding author. Tel.: +1 701 231 6254; fax: +1 701 231 8831.
** Corresponding author. Tel.: +86 25 83172358; fax: +86 25 83587428.
E-mail addresses: zhuhj@njut.edu.cn (H. Zhu), Wenfang.Sun@ndsu.edu (W. Sun).

1010-6030/$ – see front matter © 2012 Elsevier B.V. All rights reserved.
http://dx.doi.org/10.1016/j.jphotochem.2012.04.021

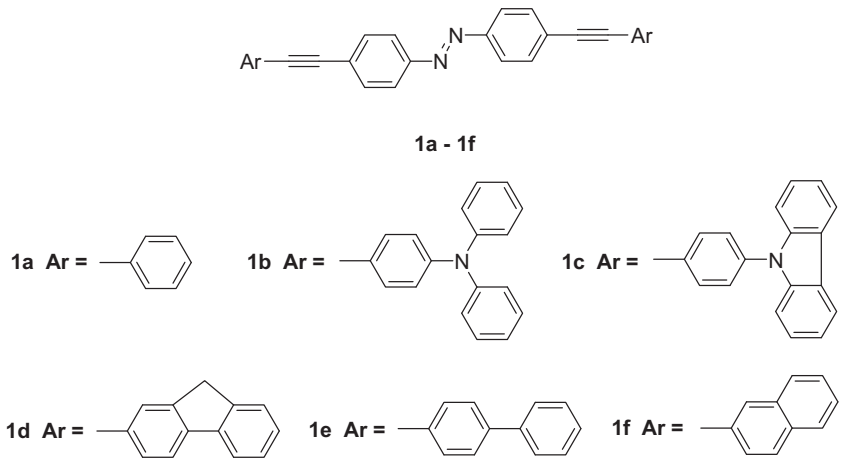

Chart 1. Structures of 4,4′-diethynylazobenzene derivatives terminally capped with substituted aromatic rings (**1a**–**1f**).

the structure–property correlations and developing new organic nonlinear absorbing materials. Compared to the platinum terdentate/bidentate nonlinear absorbing materials developed by our group [21–24], the azobenzene compounds have the advantage of synthetic convenience and low cost.

The synthesis and structural characterization details of these compounds have been reported previously [25]. In this work, we focus on the photophysical studies and the nonlinear absorption of these compounds for ns laser pulses.

2. Experimental

2.1. Photophysical measurements

A Shimadzu UV-2501 spectrophotometer was used to measure the UV–Vis absorption spectra; and a SPEX fluorolog-3 fluorometer/phosphorometer was utilized to obtain the steady-state emission spectra in different solvents (HPLC grade). The emission quantum yields were determined by the comparative method [26], in which an aqueous solution of quinine bisulfate (Φ_{em} = 0.546, λ_{ex} = 365 nm) [27] was used as the reference. An Edinburgh LP920 laser flash photolysis spectrometer was used to measure the triplet excited-state lifetimes, the triplet transient difference absorption (TA) spectra, the triplet excited-state quantum yields and the molar extinction coefficients in degassed solutions. The excitation source was the third harmonic output (355 nm) of a Nd:YAG laser (Quantel Brilliant, pulsewidth ~4.1 ns, repetition rate was set at 1 Hz). Each sample was purged with Ar for 30 min prior to measurement. Because the azobenzene molecules can undergo *trans–cis* isomerization under UV/visible light irradiation, special care was taken for each of the photophysical measurement. Each of the sample solution was freshly prepared and kept in dark before the photophysical measurement. Each of the UV–Vis and emission measurement was completed in ~30 s, thus no *trans–cis* isomerization occurred in such a short period of time, and the obtained spectra are all for the *trans* isomers. Even if for the TA spectral measurement that took approximately 30 min, the *trans–cis* isomerization in toluene solution was negligible.

Singlet depletion method [28] was applied to obtain the triplet excited-state molar extinction coefficients (ε_T) at the TA band maximum, in which ε_T was calculated by the following equation [28]:

$$\varepsilon_T = \frac{\varepsilon_S[\Delta OD_T]}{\Delta OD_S}$$

where ε_S is the ground-state molar extinction coefficient at the wavelength of the bleaching band minimum in TA spectrum; ΔOD_S and ΔOD_T are the optical density changes at the minimum of the bleaching band and the maximum of the positive band, respectively. When the ε_T value is obtained, the triplet excited-state quantum yield can be calculated by the relative actinometry [29], in which SiNc in benzene was used as the reference (ε_{590} = 70,000 M^{-1} cm^{-1}, Φ_T = 0.20) [30].

2.2. DFT calculations

To understand the nature of the ground state and the low-lying excited states, quantum chemical calculations were performed for compounds **1a**–**1f**. All calculations were conducted at the DFT level of theory, in conjunction with the B3LYP functional [31,32] and the 6-31G* basis set [33–37], as implemented in the Gaussian 09 program package [38]. In this work, geometry optimization and the frontier molecular orbitals were simulated for each of the compound.

2.3. Nonlinear transmission measurement

The nonlinear transmission experiments for compounds **1a**–**1f** at 532 nm were carried out in CH_2Cl_2 solution in a 2-mm cuvette using 4.1 ns laser pulses. The experimental setup and details were described previously [39]. The light source was the second harmonic output (λ = 532 nm) of a 4.1 ns (fwhm), 10 Hz, Q-switched Quantel Brilliant Nd:YAG laser. An *f* = 40 cm plano-convex lens was used to focus the laser beam to the center of a 2-mm-thick sample cuvette. The linear transmission of the solution was adjusted to 80%. Two Molectron J4-09 pyroelectric probes and an EPM2000 energy/power meter were used to monitor the incident and output energies.

3. Results and discussion

3.1. Electronic absorption

The UV–Vis absorption spectra of **1a**–**1f** in toluene solution at room temperature are shown in Fig. 1, and the band maxima and molar extinction coefficients for each compound are compiled in Table 1. The absorptions of **1a**–**1f** obey Lambert–Beer's law in 1×10^{-6} to 1×10^{-4} mol/L range, suggesting no ground-state aggregation or oligomerization occurs in this concentration range. The intense absorption bands below 400 nm and the broad, weak absorption band between 400 and 500 nm are

Table 1
Photophysical data for **1a**–**1f**.

	λ_{abs}/nm (ε/10^3 L mol^{-1} cm^{-1})[a]	λ_{em}/nm (Φ_{em}) R.T.[b]	λ_{em}/nm 77 K[c]	λ_{T1-Tn}/nm (τ_{TA}/μs; ε_{T1-Tn}/10^4 L mol^{-1} cm^{-1}; Φ_T)[d]
1a	385 (38.1), 495 (1.7)	401 (0.014)	384	490 (16.3, 1.87, 0.037)
1b	347 (35.8), 434 (12.2)	419 (0.064)	423	[e]
1c	293 (36.4), 370 (39.8), 489 (2.0)	392 (0.046)	386	[e]
1d	350 (41.3), 376 (41.1), 479 (1.8)	415 (0.12)	380, 404, 415	580 (12.8, 11.01, 0.34)
1e	335 (35.5), 355 (34.3), 456 (1.4)	374 (0.34)	370, 392, 423	560 (13.4, 10.43, 0.46)
1f	334 (54.7), 359 (42.8), 448 (1.6)	369 (0.25)	346, 365, 376	495 (14.4, 9.60, 0.37)

[a] Electronic absorption band maxima and molar extinction coefficients in toluene at room temperature.
[b] Room temperature emission band maxima measured in toluene at a concentration of 1×10^{-5} mol/L. Aqueous solution of quinine bisulfate (Φ_{em} = 0.546, excited at 365 nm) was used as the reference.
[c] In BuCN at a concentration of 1×10^{-5} mol/L.
[d] ns TA band maximum, triplet extinction coefficient, triplet excited-state lifetime and quantum yield measured in toluene. SiNc in C_6H_6 was used as the reference (ε_{590} = 70,000 L mol^{-1} cm^{-1}, Φ_T = 0.20).
[e] Signal too weak to be measured.

attributed to the $^1\pi,\pi^*$ and $^1n,\pi^*$ electronic transitions, respectively [3,14,17,40]. Compared to the ground-state absorption of 4,4′-diethynylazobenzene [17] (*i.e.* the parent compound), compounds **1a**–**1f** with end-capped aromatic rings exhibit a significant increase of the absorption coefficients and the $^1\pi,\pi^*$ transition bands bathochromically shift. The minor solvent effect as exemplified in Fig. 2 for **1b** and in Supporting information Figs. S1–S5 supports the $^1\pi,\pi^*$ assignment for the major absorption band(s). However, except for **1a**, the other five compounds all possess a shoulder at the longer wavelength side of the $^1\pi,\pi^*$ transition band(s). With reference to the DFT calculation that will be discussed later, this shoulder could be attributed to an intramolecular charge transfer (^{1}ICT) transition from the terminal aromatic rings to the central azobenzene component, which is more prominent for **1b** that possesses strong electron-donating NPh_2 substituents on the terminal benzene rings. It was reported that *trans* to *cis* isomerization could occur under 365 nm irradiation for the azobenzene compounds, and the ICT band increased when the isomerization occurs [25]. However, in all of our UV–Vis experiment, the sample solutions were freshly prepared and each spectral measurement took only ~30 s. Therefore, no observable *trans–cis* isomerization occurred in such a short period of time. The ICT band should be attributed to the *trans* isomers. In addition, compared to the absorption spectrum of the parent 4,4′-diethynylazobenzene compound reported in the literature [17], the characteristic $^1n,\pi^*$ bands observed in the parent azobenzene are no longer distinguishable in **1b** because the $^1n,\pi^*$ band is buried in the ICT absorption band.

The absorption bands of **1a**–**1f** are influenced significantly by the end-capped aromatic rings. Compared to the phenyl-capped compound **1a**, strong electron-donating substituent NPh_2 causes a pronounced separation of the $^1\pi,\pi^*$ transition and the ^{1}ICT transition in **1b**, with a bathochromic shift of the ^{1}ICT band and hypsochromic shift of the $^1\pi,\pi^*$ band. In contrast, when π-conjugation of the end-capped aromatic ring increases, as in compounds **1d**–**1f**, the whole absorption spectrum is blue-shifted, with the ^{1}ICT transition appearing as a shoulder at the longer wavelength.

To gain insight into the nature of the ground electronic state and the low-lying singlet excited electronic state, density functional theory (DFT) calculations on **1a**–**1f** in gas phase were performed. The ground-state geometries of **1a**–**1f** were fully optimized using DFT at the B3LYP/6-31G* level, as implemented in the Gaussian 09 program package. Fig. 3 illustrates the optimized structures, and the electron density distribution of the HOMO and LUMO for compounds **1a**–**1f**. The excitation energy (eV), wavelength (nm), oscillator strength, dominant contributing configuration, and the associated configuration coefficient of several low-lying electronic states of compounds **1a**–**1f** are listed in Supporting information Tables S1–S6, and the contour plots of several other frontier molecular orbitals for compounds **1a**–**1f** are depicted in Supporting information Figs. S6–S11. As shown in Fig. 3, the aryleneethynyleneazobenzene backbone is almost coplanar, while the substituents

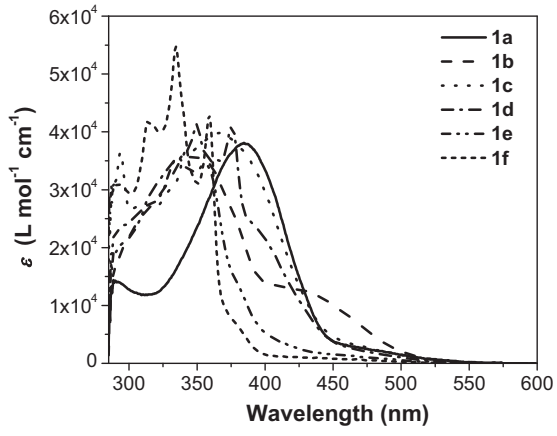

Fig. 1. UV–Vis absorption spectra of **1a**–**1f** in toluene.

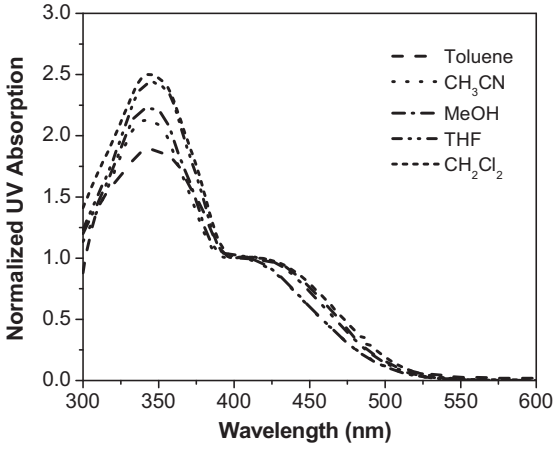

Fig. 2. Normalized UV–Vis absorption spectra of **1b** in different solvents. The concentration of the solution was adjusted in order to obtain $A_{365\,nm}$ = 0.08 in a 1-cm cuvette. The spectra are normalized to the low-energy charge-transfer band.

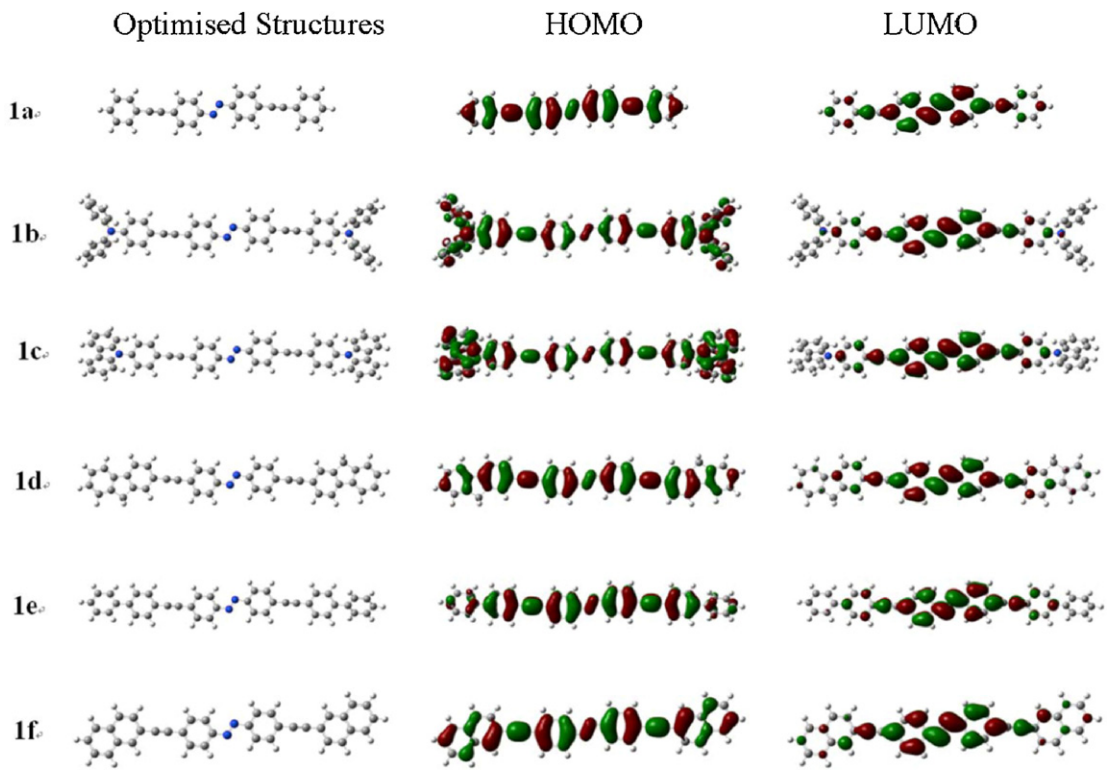

Fig. 3. Optimized geometry and contour plots of electron density distribution of HOMO and LUMO of compounds **1a–1f** in gas phase calculated using DFT at the B3LYP/6-31G* level.

at the terminal aryl motifs are twisted away from the aryleneethynyleneazobenzene backbone.

Due to the nearly coplanar geometry, the π-electrons in the HOMO of **1a–1f** are delocalized over the entire phenyleneethynyleneazobenzene backbone; while their LUMO is localized on the diethynylazobenzene core. Therefore, the HOMO → LUMO transition that is the dominant contributing configuration to the S_1 state in **1a–1f** should be ascribed to a mixture of π,π^* and ICT characters, which is consistent with our analysis of the low-energy absorption shoulder in the UV–Vis spectra. The calculated energy values and relative energy band gaps (E_g) are presented in Table 2. The results clearly demonstrate that strong electron-donating substituent, such as NPh_2 in **1b**, increases the energy level of HOMO more than that of LUMO, thus the HOMO–LUMO gap decreases, causing a red-shift of the π,π^*/ICT band. In contrast, extension of the π-conjugation of the end-capped aryl group increases the energy of LUMO more than that of the HOMO, resulting in a salient blue-shift of the π,π^*/ICT band. This trend follows that observed from the UV–Vis absorption measurement.

3.2. Emission

The emission characteristics of compounds **1a–1f** in a variety of solvents were investigated at room temperature. The normalized emission spectra of these compounds in toluene at a concentration of 1×10^{-5} mol/L are illustrated in Fig. 4. The emission band maxima and quantum yields are listed in Table 1. Excitation of these compounds at their respective absorption band maximum at room temperature results in structured violet to blue luminescence, as shown in Fig. 4 and Table 1. The Stokes shifts of these compounds are quite small and the emission lifetimes are too short (<5 ns) to be measured on our instrument. Taking these features into account, we can assign the observed emission to the $^1\pi,\pi^*$ state. The weak emission of these compounds could be attributed to the twisting of the emitting state by the azobenzene unit, which is in accordance with the properties of azobenzenes reported in the literature [3,6,13,17,40]. In addition, the emission of these compounds is not affected by the excitation wavelength, as exemplified for sample **1b** in Fig. S12, indicating that no measurable *trans–cis* isomerization occurs during the emission measurement.

Table 2
HOMO and LUMO energy values theoretically calculated for molecules **1a–1f** in gas phase.

	1a	1b	1c	1d	1e	1f
LUMO (eV)	−2.87	−2.38	−2.66	−2.50	−2.54	−2.55
HOMO (eV)	−5.51	−4.89	−5.32	−5.27	−5.41	−5.40
E_g (eV)	2.64	2.51	2.66	2.77	2.87	2.85

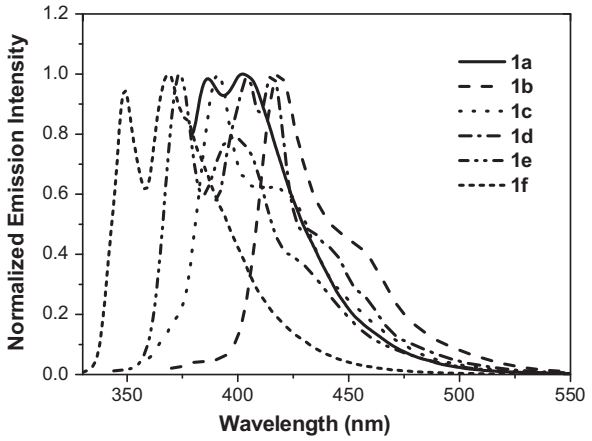

Fig. 4. Normalized emission spectra of **1a–1f** in toluene solution ($c = 1 \times 10^{-5}$ mol/L). The excitation wavelength was 340 nm for **1a**, 360 nm for **1b**, 350 nm for **1c**, **1d** and **1f**, and 320 nm for **1f**.

Table 3
Emission energy and quantum yield of **1a**–**1f** in different solvents at R.T.

	λ_{em}/nm (Φ_{em}[a])			
	Toluene	THF	CH_2Cl_2	CH_3CN
1a	401 (0.014)	[b]	421 ([c])	395 ([c])
1b	419 (0.064)	425 (0.016)	436 (0.013)	443 (0.010)
1c	392 (0.046)	[b]	412 (0.012)	439 ([c])
1d	415 (0.12)	412 (0.055)	413 (0.044)	410 (0.037)
1e	374 (0.34)	373 (0.27)	373 (0.20)	370 (0.18)
1f	369 (0.25)	369 (0.21)	368 (0.18)	367 (0.17)

[a] A degassed aqueous solution of quinine bisulfate (Φ_{em} = 0.546, excited at 365 nm) was used as the reference.
[b] Signal too weak to be measured.
[c] Φ_{em} < 0.01.

Except for **1b** and **1c**, all of the other compounds exhibit minor solvatochromic effect (Supporting information Figs. S13–S17), indicating that the emitting state for **1a** and **1d**–**1f** has predominant $^1\pi,\pi^*$ character. The emission energies and quantum yields of **1a**–**1f** in different solvents are summarized in Table 3. For compounds **1b** and **1c**, both of them exhibit a positive solvatochromic effect (exemplified in Fig. 5 for **1b** and in Supporting information Fig. S14 for **1c**), when the dielectric constant (ε) of the solvent increases, the emission energy of the compound decreases. As shown in Fig. 5, in low-polarity solvents, such as toluene (ε = 2.38) and THF (ε = 7.39), a slight vibronic structure is observed with a vibronic spacing of approximately 1940 cm^{-1}, which is consistent with the stretching mode of the C≡C bond. Therefore, the emitting state in low-polarity solvent could be ascribed to the $^1\pi,\pi^*$ state that is mainly localized on the diethynylazobenzene backbone. On the other hand, in more polar solvents, such as CH_2Cl_2 (ε = 8.90) and CH_3CN (ε = 37.5), the emission band is red-shifted and becomes structureless. This suggests that the emitting state in more polar solvent is likely dominated by a charge transfer state, *i.e.* the ^{1}ICT state. This feature is commonly seen from compounds with charge transfer character. Polar solvent can stabilize the charge transfer ^{1}ICT state better than the $^1\pi,\pi^*$ state, therefore the ^{1}ICT state becomes the lowest excited state and emits in polar solvents. Similar phenomenon was observed for compound **1c**. The drastic solvatochromic effect observed in **1b** and **1c** but not in the other compounds should be attributed to the electron-donating group, *i.e.* NPh_2 and carbazolyl in these two compounds, which enhances electron transfer from the end of the molecule to the azobenzene motif. On the other hand, when the π-conjugation of the terminal aromatic ring increases, such as the case in **1d**, **1e** and **1f**, the π-electrons are delocalized over the whole molecule and thus $^1\pi,\pi^*$ state is more stabilized; and minor solvatochromic effect is observed. The dominant $^1\pi,\pi^*$ nature of the emitting state in **1d**, **1e** and **1f** is also reflected by the increased emission quantum yields compared to those in **1a**, **1b** and **1c**. In addition, Lippert-Mataga plots were created to describe the solvatochromic shifts ($\Delta\bar{\nu}$ in cm^{-1}) as a function of the Lippert solvent parameter $\Delta f = f(\varepsilon) - f(n^2)$ upon excitation, which are exemplified in Fig. S18 for **1b** and in Fig. S19 for **1e**. The linear relationship of the Stokes shift (cm^{-1}) *versus* Δf confirms that no *trans*-to-*cis* configuration change is observed in these molecules after excitation [41].

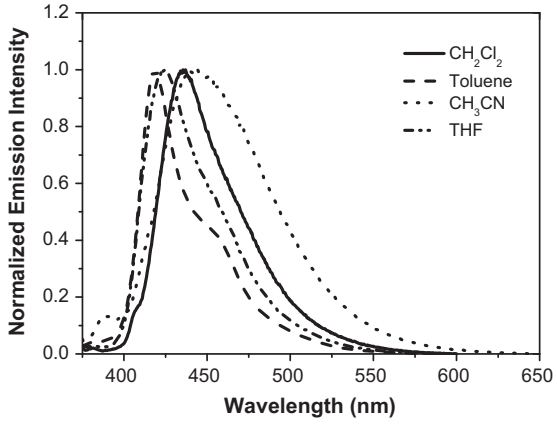

Fig. 5. Normalized emission spectra of **1b** in different solvents. The excitation wavelength was 365 nm.

3.3. Triplet transient difference absorption

Transient difference absorption (TA) spectral measurement gives rise to the absorption difference between the ground state and the excited state. A positive band in a TA spectrum indicates stronger excited-state absorption than that of the ground state, while a negative band (bleaching band) suggests stronger ground-state absorption than that of the excited state. It can predict the spectral region where reverse saturable absorption (*i.e.* transmission decreases when incident fluence increases) may occur. In addition, from the decay of the transient absorption, the lifetime of the excited state giving rise to the excited-state absorption can be obtained. Fig. 6 displays the time-resolved triplet TA spectra of **1a**, **1d**, **1e**, and **1f** in degassed toluene solution. The TA absorption band maxima, the triplet excited-state lifetime deduced from the decay of the TA, the triplet excited-state absorption coefficient, and the triplet quantum yield for these compounds are listed in Table 1. The TA spectra of **1b** and **1c** were unable to be measured, probably due to the stronger charge-transfer character in these two compounds, which could quench the $^3\pi,\pi^*$ state.

The triplet lifetimes deduced from the decay of the TA of compounds **1d**–**1f** are very long, *i.e.* ~10 μs in toluene, while the lifetimes are too weak to be measured in polar solvents, such as CH_3CN. The long triplet lifetime in toluene suggests that the excited state giving rise to the transient absorption is likely to be dominated by the $^3\pi,\pi^*$ state, although the contribution from the ^{3}ICT state cannot be completely ruled out. However, polar solvents can facilitate the ICT, which causes the quench of the $^3\pi,\pi^*$ state and consequently diminishes the transient absorption.

Comparing the TA spectra of **1a**, **1d**, **1e** and **1f**, it is obvious that the shape and intensity of the transient absorption are significantly influenced by the end-capped aromatic rings. As mentioned earlier, electron-donating substituents on the terminal aromatic rings, such as NPh_2 in **1b** and carbazolyl in **1c**, enhance the ICT and thus quench the TA from the $^3\pi,\pi^*$ state. On the contrary, when the π-conjugation of the terminal aromatic ring increases in **1d**, **1e** and **1f**, the TA band is bathochromically shifted, accompanied by a drastically enhanced triplet excited-state molar extinction coefficient and a much higher triplet quantum yield. These characteristics support that the absorbing excited state is predominantly a $^3\pi,\pi^*$ state, likely localized on the terminal arylethynyl motif.

3.4. Reverse saturable absorption

The UV–Vis absorption spectra of **1a**–**1f** show that these compounds have very weak ground-state absorption above 500 nm, while the triplet excited-state absorbs from 450 nm to 700 nm (see the TA spectra in Fig. 6). Therefore, reverse saturable absorption (RSA, *i.e.* absorptivity of the compound increases with increased incident fluence) is expected to occur in this spectral region. To demonstrate this, nonlinear transmission experiment was carried out using 4.1 ns laser pulses at 532 nm and the result is illustrated in Fig. 7. With increased incident fluence, the transmission of **1a**–**1f** decreases. At high incident fluence of ~3.3 J/cm^2,

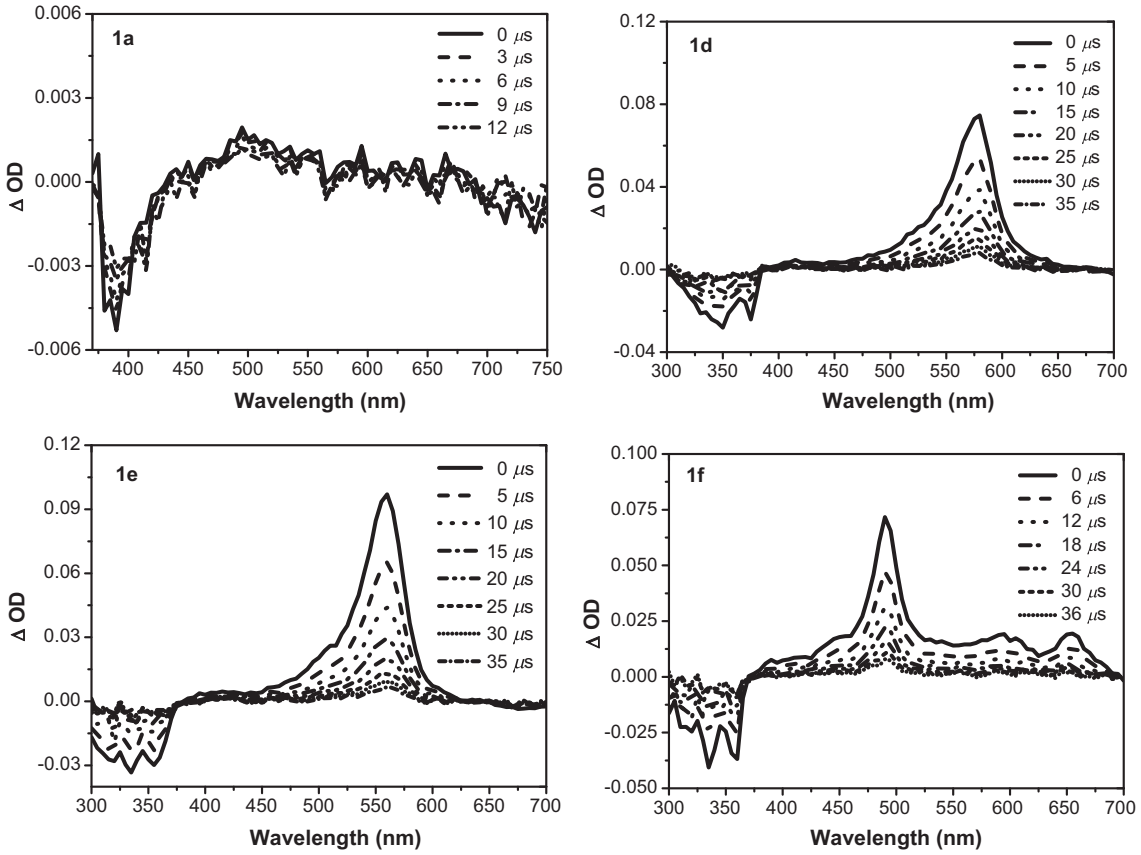

Fig. 6. Time-resolved triplet transient difference absorption spectrum of **1a**, **1d**, **1e** and **1f** in toluene. λ_{ex} = 355 nm. A_{355} = 0.4 in a 1-cm cuvette.

their transmissions all drop from 80% to lower than 60%, which clearly manifests the RSA at 532 nm. The strength of the RSA for these compounds follows the trend of **1b** > **1c** ≈ **1a** > **1e** > **1f** > **1d**. Among these, **1b** exhibits the strongest RSA, with a RSA threshold (defined as the incident fluence at which point the transmittance drops to 70% of the linear transmittance) of 1.8 J/cm^2 and the transmission decreases to 0.39 when the incident fluence reaches 3.3 J/cm^2. The ground-state absorption cross sections at 532 nm for these compounds are listed in Table 4, which are deduced from the ε values obtained from their UV–Vis absorption spectra and the conversion equation $\sigma = 2303\varepsilon/N_A$, where N_A is the Avogadro constant. The triplet excited-state absorption cross sections at 532 nm are estimated from the ΔOD at zero time delay and the ε_{T1-Tn} at the TA band maximum. The σ_{ex}/σ_0 value follows this trend: **1e** > **1f** > **1d** > **1a**. This trend implies that increasing the π-conjugation of the terminal aromatic rings could reduce the ground-state absorption cross section while improving the triplet excited-state absorption cross section, which results in a larger ratio of σ_{ex}/σ_0. The σ_{ex}/σ_0 ratio for **1b** and **1c** cannot be estimated because the triplet TA for these two compounds was too weak to be measured. It is noted that the observed RSA trend is different from that of σ_{ex}/σ_0 for **1a**. This indicates that the triplet excited-state absorption might not be the dominant contributor to the nonlinear absorption at ns regime for **1a**, which is consistent with its very low triplet quantum yield. Singlet excited-state absorption could play a significant role for **1a**. Unfortunately, the singlet excited-state TA spectra are currently unavailable because of the lack of appropriate instrument in our laboratory. We speculate that the strong RSA for **1a**–**1c** likely arise from their singlet excited-state absorption.

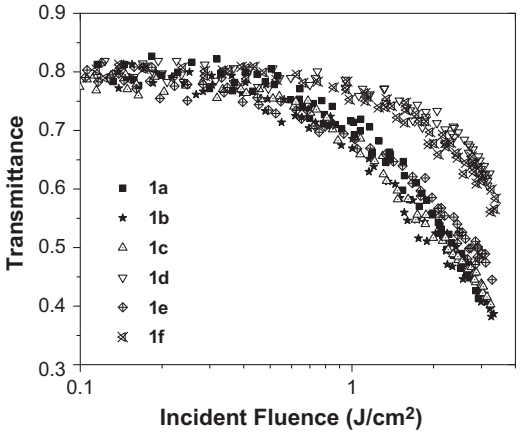

Fig. 7. Transmittance *versus* incident fluence curves for **1a**–**1f** in toluene for 4.1 ns laser pulses at 532 nm. The linear transmission was adjusted to 80% for each sample in a 2-mm cell.

Table 4
Ground-state (σ_0) and excited-state (σ_{ex}) absorption cross sections of compounds **1a** and **1d**–**1f** in toluene at 532 nm.

	1a	1d	1e	1f
$\sigma_0/10^{-18}$ cm^2	1.91	1.15	0.76	0.38
$\sigma_{ex}/10^{-18}$ cm^2	28.9	136.6	202.3	82.0
σ_{ex}/σ_0	15.2	119	264	214
$\Phi_T\sigma_{ex}/\sigma_0$	1.2	40.0	122	80.0

4. Conclusion

The photophysics of 4,4′-diethynylazobenzene derivatives terminally capped with substituted aromatic rings (**1a**–**1f**) were systematically investigated. The ^{1}ICT and $^1\pi,\pi^*$ absorption bands are blue-shifted when the π-conjugation of the terminally capped aromatic rings increases; while strong electron-donating substituent NPh_2 causes a red-shift of the ^{1}ICT/$^1\pi,\pi^*$ band. All compounds exhibit violet to blue $^1\pi,\pi^*$/^{1}ICT emission, but the fluorescence quantum yields for **1d**–**1f** are drastically higher than the other compounds due to enhanced $^1\pi,\pi^*$ character in these three compounds. For the similar reason, compounds **1d**–**1f** exhibit stronger triplet $^3\pi,\pi^*$ excited-state absorption in the visible region, accompanied by a relatively long triplet excited-state lifetime. All the compounds exhibit reverse saturable absorption for ns laser pulses at 532 nm, with the RSA strength decreases following the trend of **1b** > **1c** ≈ **1a** > **1e** > **1f** > **1d**.

Acknowledgments

W. Sun acknowledges the financial support from the National Science Foundation (CAREER CHE-0449598). H. Zhu acknowledge the National High Technology Research and Development Program ("863" Program) of China (2009AA032901).

Appendix A. Supplementary data

Supplementary data associated with this article can be found, in the online version, at http://dx.doi.org/10.1016/j.jphotochem.2012.04.021.

References

[1] Y. Shirai, T. Sasaki, J.M. Guerrero, B.-C. Yu, P. Hodge, J.M. Tour, Synthesis and photoisomerization of fullerene- and oligo(phenylene ethynylene)-azobenzene derivatives, ACS Nano 2 (2008) 97–106.
[2] Y. Furusho, Y. Tanaka, T. Maeda, M. Ikeda, E. Yashima, Photoresponsive double-stranded helices composed of complementary strands, Chemical Communications (2007) 3174–3176.
[3] L.-X. Liao, F. Stellacci, D.V. McGrath, Photoswitchable flexible and shape-persistent dendrimers: comparison of the interplay between a photochromic azobenzene core and dendrimer structure, Journal of the American Chemical Society 126 (2004) 2181–2185.
[4] K. Okano, O. Tsutsumi, A. Shishido, T. Ikeda, Azotolane liquid-crystalline polymers: huge change in birefringence by photoinduced alignment change, Journal of the American Chemical Society 128 (2006) 15368–15369.
[5] F.O. Koller, C. Sobotta, T.E. Schrader, T. Cordes, W.J. Schreier, A. Sieg, P. Gilch, Slower processes of the ultrafast photo-isomerization of an azobenzene observed by IR spectroscopy, Chemical Physics 341 (2007) 258–266.
[6] D. Grebel-Koehler, D. Liu, S. De Feyter, V. Enkelmann, T. Weil, C. Engels, C. Samyn, K. Mullen, F.C. De Schryver, Synthesis and photomodulation of rigid polyphenylene dendrimers with an azobenzene core, Macromolecules 36 (2003) 578–590.
[7] Z. Yu, S. Hecht, Reversible and quantitative denaturation of amphiphilic oligo(azobenzene) foldamers, Angewandte Chemie International Edition 50 (2011) 1640–1643.
[8] M.-M. Russew, S. Hecht, Photoswitches: from molecules to materials, Advanced Materials 22 (2010) 3348–3360.
[9] S. Yagai, A. Kitamura, Recent advances in photoresponsive supramolecular self-assemblies, Chemical Society Reviews 37 (2008) 1520–1529.
[10] H. Yamada, Y. Furusho, H. Ito, E. Yashima, Complementary double helix formation through template synthesis, Chemical Communications 46 (2010) 3487–3489.
[11] M.M.M. Raposo, A.M.C. Fonseca, M.C.R. Castro, M. Belsley, M.F.S. Cardoso, L.M. Carvalho, P.J. Coelho, Synthesis and characterization of novel diazenes bearing pyrrole, thiophene and thiazole heterocycles as efficient photochromic and nonlinear optical (NLO) materials, Dyes and Pigments 91 (2011) 62–73.
[12] Z. Chen, S. Dong, C. Zhong, Z. Zhang, L. Niu, Z. Li, F. Zhang, Photoswitching of the third-order nonlinear optical properties of azobenzene-containing phthalocyanines based on reversible host-guest interactions, Journal of Photochemistry and Photobiology A: Chemistry 206 (2009) 213–219.
[13] X. Xia, L.H. Gan, X. Hu, The synthesis and properties of novel, functional azobenzene based metal complexes, Dyes and Pigments 83 (2009) 291–296.
[14] S. Zarwell, K. Ruck-Braun, Synthesis of an azobenzene-linker-conjugate with tetrahedrical shape, Tetrahedron Letters 49 (2008) 4020–4025.
[15] T. Sasaki, J.M. Tour, Synthesis of a new photoactive nanovehicle: a nanoworm, Organic Letters 10 (2008) 897–900.
[16] Y. Morishima, M. Tsuji, M. Kamachi, K. Hatada, Photochromic isomerization of azobenzene moieties compartmentalized in hydrophobic microdomains in a microphase structure of amphiphilic polyelectrolytes, Macromolecules 25 (1992) 4406–4410.
[17] J. Zeitouny, C. Aurisicchio, D. Bonifazi, R.D. Zorzi, S. Geremia, M. Bonini, C.-A. Palma, P. Samorì, A. Listorti, A. Belbakrab, N. Armaroli, Photoinduced structural modifications in multicomponent architectures containing azobenzene moieties as photoswitchable cores, Journal of Materials Chemistry 19 (2009) 4715–4724.
[18] J. Zeitouny, A. Belbakra, A. Llanes-Pallas, A. Barbieri, N. Armaroli, D. Bonifazi, On the route to mimic natural movements: synthesis and photophysical properties of a molecular arachnoid, Chemical Communications 47 (2011) 451–453.
[19] B.-C. Yu, Y. Shirai, J.M. Tour, Syntheses of new functionalized azobenzenes for potential molecular electronic devices, Tetrahedron 62 (2006) 10303–10310.
[20] A.K. Flatt, S.M. Dirk, J.C. Henderson, D.E. Shen, J. Su, M.A. Reed, J.M. Tour, Synthesis and testing of new end-functionalized oligomers for molecular electronics, Tetrahedron 59 (2003) 8555–8570.
[21] W. Sun, B. Zhang, Y. Li, T.M. Pritchett, Z. Li, J.E. Haley, Broadband nonlinear absorbing platinum 2,2′-bipyridine complex bearing 2-(benzothiazol-2′-yl)-9,9-diethyl-7-ethynylfluorene ligands, Chemistry of Materials 22 (2010) 6384–6392.
[22] R. Liu, Y. Li, Y. Li, H. Zhu, W. Sun, Photophysics and nonlinear absorption of cyclometalated 4,6-diphenyl-2,2′-bipyridyl platinum(II) complexes with different acetylide ligands, Journal of Physical Chemistry A 114 (2010) 12639–12645.
[23] P. Shao, Y. Li, J. Yi, T.M. Pritchett, W. Sun, Cyclometalated platinum(II) 6-phenyl-4-(9,9-dihexylfluoren-2-yl)-2,2′-bipyridine complexes: synthesis, photophysics, and nonlinear absorption, Inorganic Chemistry 49 (2010) 4507–4517.
[24] P. Shao, Y. Li, A. Azenkeng, M.R. Hoffmann, W. Sun, Influence of alkoxyl substituent on 4,6-diphenyl-2,2′-bipyridine ligand on photophysics of cyclometalated platinum(II) complexes: admixing intraligand charge transfer character in low-lying excited states, Inorganic Chemistry 48 (2009) 2407–2419.
[25] R. Liu, Q. Xiao, Y. Li, H. Chen, Z. Yan, H. Zhu, Phenylene ethynylene azobenzenes with symmetrical peripheral chromophores: synthesis, optical properties and photoisomerization behaviors study, Dyes and Pigments 92 (2011) 626–632.
[26] G.A. Crosby, J.N. Demas, Measurement of photoluminescence quantum yields. Review, Journal of Physical Chemistry 75 (1971) 991–1024.
[27] W.H. Melhuish, Quantum efficiencies of fluorescence of organic substances: effect of solvent and concentration of the fluorescent solute 1, Journal of Physical Chemistry 65 (1961) 229–235.
[28] I. Carmichael, G.L.J. Hug, Triplet–triplet absorption spectra of organic molecules in condensed phases, Journal of Physical and Chemical Reference Data 15 (1986) 1–250.
[29] C.V. Kumar, L. Qin, P.K. Das, Aromatic thioketone triplets and their quenching behaviour towards oxygen and di-t-butylnitroxy radical. A laser-flash-photolysis study, Journal of the Chemical Society, Faraday Transactions 2: Molecular and Chemical Physics 80 (1984) 783–793.
[30] P.A. Firey, W.E. Ford, J.R. Sounik, M.E. Kenney, M.A.J. Rodgers, Silicon naphthalocyanine triplet state and oxygen. A reversible energy-transfer reaction, Journal of the American Chemical Society 110 (1988) 7626–7630.
[31] D.B. Axel, Density-functional thermochemistry. III. The role of exact exchange, Journal of Chemical Physics 98 (1993) 5648–5652.
[32] C. Lee, W. Yang, R.G. Parr, Development of the Colle–Salvetti correlation-energy formula into a functional of the electron density, Physical Review B 37 (1988) 785–789.
[33] T. Clark, J. Chandrasekhar, G.W. Spitznagel, P.v.R. Schleyer, Efficient diffuse function-augmented basis sets for anion calculations. III. The 3-21 + G basis set for first-row elements, lithium to fluorine, Journal of Computational Chemistry 4 (1983) 294–301.
[34] M.M. Francl, W.J. Pietro, W.J. Hehre, J.S. Binkley, M.S. Gordon, D.J. DeFrees, J.A. Pople, Self-consistent molecular orbital methods. XXIII. A polarization-type basis set for second-row elements, Journal of Chemical Physics 77 (1982) 3654–3665.
[35] P.M.W. Gill, B.G. Johnson, J.A. Pople, M.J. Frisch, The performance of the Becke–Lee–Yang–Parr (B-LYP) density-functional theory with various basis sets, Chemical Physics Letters 197 (1992) 499–505.
[36] P.C. Hariharan, J.A. Pople, Influence of polarization functions on MO hydrogenation energies, Theoretica Chimica Acta 28 (1973) 213–222.
[37] R. Krishnan, J.S. Binkley, R. Seeger, J.A. Pople, Self-consistent molecular orbital methods. A basis set for correlated wave functions, Journal of Chemical Physics 72 (1980) 650–654.
[38] M.J. Frisch, G.W. Trucks, H.B. Schlegel, G.E. Scuseria, M.A. Robb, J.R. Cheeseman, J.A. Montgomery Jr., T. Vreven, K.N. Kudin, J.C. Burant, J.M. Millam, S.S. Iyengar, J. Tomasi, V. Barone, B. Mennucci, M. Cossi, G. Scalmani, N. Rega, G.A. Petersson, H. Nakatsuji, M. Hada, M. Ehara, K. Toyota, R. Fukuda, J. Hasegawa, M. Ishida, T. Nakajima, Y. Honda, O. Kitao, H. Nakai, M. Klene, X. Li, J.E. Knox, H.P. Hratchian, J.B. Cross, V. Bakken, C. Adamo, J. Jaramillo, R. Gomperts, R.E. Stratmann, O. Yazyev, A.J. Austin, R. Cammi, C. Pomelli, J.W. Ochterski, P.Y. Ayala, K. Morokuma, G.A. Voth, P. Salvador, J.J. Dannenberg, V.G. Zakrzewski, S. Dapprich, A.D. Daniels, M.C. Strain, O. Farkas, D.K. Malick, A.D. Rabuck, K. Raghavachari, J.B. Foresman, J.V. Ortiz, Q. Cui, A.G. Baboul, S. Clifford, J. Cioslowski, B.B. Stefanov, G. Liu, A. Liashenko, P. Piskorz, I. Komaromi, R.L. Martin, D.J. Fox, T. Keith,

M.A. Al-Laham, C.Y. Peng, A. Nanayakkara, M. Challacombe, P.M.W. Gill, B. Johnson, W. Chen, M.W. Wong, C. Gonzalez, J.A. Pople, Gaussian 03, revision C.02, Gaussian, Inc, Wallingford, CT, 2004.
[39] W. Sun, H. Zhu, P.M. Barron, Binuclear cyclometalated platinum(II) 4,6-diphenyl-2,2′-bipyridine complexes: interesting photoluminescent and optical limiting materials, Chemistry of Materials 18 (2006) 2602–2610.
[40] W. Freyer, D. Brete, R. Schmidt, C. Gahl, R. Carley, M. Weinelt, Switching behavior and optical absorbance of azobenzene-functionalized alkanethiols in different environments, Journal of Photochemistry and Photobiology A: Chemistry 204 (2009) 102–109.
[41] W. Qin, M. Baruah, M. Sliwa, M. Van der Auweraer, W.M. De Borggraeve, D. Beljonne, B. Van Averbeke, N. Boens, Ratiometric, fluorescent BODIPY dye with aza crown ether functionality: synthesis, solvatochromism, and metal ion complex formation, Journal of Physical Chemistry A 112 (2008) 6104–6114.